Water's Role in Reshaping a Macrocycle's Binding Pocket: Infrared and Ultraviolet Spectroscopy of Benzo-15-crown-5−$(H_2O)_n$ and 4′-aminobenzo-15-crown-5−$(H_2O)_n$, $n = 1, 2$

V. Alvin Shubert,[†] Christian W. Müller, and Timothy S. Zwier*

Purdue University, Department of Chemistry, 560 Oval Drive, West Lafayette, Indiana 47907-2084

Received: May 6, 2009

Laser-induced fluorescence (LIF), resonant two-photon ionization (R2PI), ultraviolet hole-burning (UVHB), resonant ion-dip infrared (RIDIR), and infrared-infrared ultraviolet hole-burning (IR−IR−UV) spectroscopies were carried out on benzo-15-crown-5 ether−$(H_2O)_n$ (B15C−$(H_2O)_n$) and 4′-amino-benzo-15-crown-5 ether−$(H_2O)_n$ (ABC−$(H_2O)_n$) clusters with $n = 1,2$ formed in a supersonic expansion. Two isomers of B15C−$(H_2O)_1$ with S_0-S_1 origins at 35 628 and 35 685 cm^{-1} (B15C−$(H_2O)_1$(A) and B15C−$(H_2O)_1$(B), respectively) were identified and, on the basis of the combined evidence from the single-isomer UV and IR spectra, assigned to structures in which the H_2O molecule donates both its OH groups to H-bonds to the crown oxygens. Both isomers share the same open, chairlike C_s symmetry structure for the crown ether that exposes the crown oxygen lone pairs to binding to H_2O on the interior of the crown. This crown conformation is not among those represented in the observed conformers in the absence of the H_2O molecule, indicating that even a single water molecule is capable of reshaping the crown binding pocket in binding to it. In B15C−$(H_2O)_1$(A), the water molecule takes up a position parallel to the crown plane of symmetry, using one OH group to bind to the two benzo oxygens, while the other OH binds to a single crown oxygen on the opposite side of the crown. The H_2O molecule in B15C−$(H_2O)_1$(B) binds to the other two crown oxygens, in an orientation perpendicular to the crown's symmetry plane. B15C−$(H_2O)_2$ also has two isomers. The first, B15C−$(H_2O)_2$(A) with S_0-S_1 origin at 35 813 cm^{-1}, is assigned to a structure in which the two water molecules take up the two positions occupied by individual water molecules in B15C−$(H_2O)_1$ A and B. The second isomer, with S_0-S_1 origin at 35 665 cm^{-1}, has an OH stretch RIDIR spectrum that reflects a water−water H-bond, with the second water molecule binding to the crown-bound water in the parallel binding site. The combined data from B15C−$(H_2O)_1$, ABC−$(H_2O)_1$, and ABC−(HOD) complexes is used to deduce the uncoupled OH stretch wavenumber shifts associated with each of the unique binding sites for H_2O to the crown. Arguments are presented that the binding pocket present in benzo-15-crown-5 ether is of a near ideal size to accommodate strong bidentate binding of individual water molecules to its most open crown conformation.

I. Introduction

Crown ethers have long been noted for their ability to selectively bind substrates, especially cations.[1,2] One of the hallmarks of the crown ethers is the flexibility of the macrocycle. As such, numerous studies have investigated the properties of crown ethers involving complexation to the crown cycle.[1−17] Much of this work was performed in aqueous solution, focusing on the structure and binding energy of the crown−cation complex. While it is understandable that the majority of these studies have focused on ion binding,[1,3−9] the oxygen-rich pocket is also ideally suited to binding other types of substrates,[8,10−17] including water.[10,11] From a fundamental viewpoint, the crown macrocycle can be considered a model receptor site. Since the crown ethers are often used in aqueous solution, water molecules will bind to the oxygen-rich binding pocket, effecting the properties both of the bound water and of the crown itself.

The preceding paper[18] described an investigation of the single conformation spectroscopy of two 15-crown-5 ethers under jet-cooled conditions. The conformation specific spectroscopy was used to deduce the number of conformers present and characterize, to the extent possible, the conformational geometries present in the supersonic expansion. In these crowns, the observed conformations (3 for benzo-15-crown-5 ether (B15C) and 4 for 4′-aminobenzo-15-crown-5 ether (ABC)) differed in the degree to which the macrocycle was buckled in on itself in the absence of a binding partner.

In bulk aqueous solution, it is difficult to deduce much about the effect of the solvent molecule(s) on the conformational preferences of the crown ethers. One would anticipate that the crown ethers will be good H-bond acceptors for the water OH groups, given the number of oxygen sites present in the crown. The fact that the crown possesses multiple oxygen sites in close proximity to one another raises the possibility that bound water molecules could interact with more than one site simultaneously. However, the consequences of this complexation for the crown conformation remain unclear.

Molecular clusters provide an ideal environment in which to study exactly these types of solvent effects under controlled conditions. In the present work, we extend our studies of 15-crown-5 ethers to include crown ether−$(H_2O)_n$ complexes with $n = 1,2$. This work follows a similar pathway to those in the recent studies by Kusaka et al. on benzo-18-crown-6−$(H_2O)_n$ and dibenzo-18-crown-6−$(H_2O)_n$ complexes.[10,11] As we shall see, in both B15C and ABC, the crown ether responds to the

* Author to whom correspondence should be addressed. E-mail: zwier@purdue.edu.

[†] Current address: Argonne National Laboratory, Chemical Sciences and Engineering Division, 9700 South Cass Ave., Argonne, IL 60439.

10.1021/jp904233y CCC: $40.75
Published on Web 06/24/2009

presence of even a single water molecule by opening itself up to a more symmetric structure in which multiple ether sites are configured to act as proton acceptors in H-bonds with water molecules. Furthermore, this crown conformation is poised to accommodate a double H-bonded H_2O molecule in two distinct, spectroscopically distinguishable ways, with both sites being occupied in one of the $n = 2$ clusters.

The infrared spectra of these water molecules bound to the crown ether are extremely intriguing, leading us to an isotopic study with HOD complexes. In so doing, we uncover circumstances that will be more prevalent as the size and complexity of the molecule grows and in which the "standard" double resonance methods fail to provide single-conformation spectra. To that end, we employ herein a recently introduced triple resonance method, IR−IR−UV spectroscopy, by which we obtain conformation-specific infrared spectra even in the presence of complete UV spectral overlap.[19]

II. Methods

A. Experimental Section. B15C (>99% purity) and ABC (97% purity) were used as supplied (Sigma Aldrich). For the most part, the experimental conditions and methods were very similar to those used to study the isolated crown ethers in the preceding paper.[18] UV−UV hole-burning (UVHB)[20] and infrared dip[21,22] methods were employed to obtain conformation specific electronic and infrared spectra, respectively. The transitions used as a means of single-conformation detection when obtaining both UVHB and RIDIR spectra are marked on the appropriate figures. Monohydrated crown ether complexes were present in the expansion without need for flowing buffer gas over a water reservoir, due to either the presence of a small amount of water in the gas lines or adsorption of water in the solid sample from atmospheric water vapor.

Bands associated with the crown−water complexes were identified using mass-resolved R2PI spectroscopy in a molecular beam time-of-flight mass spectrometer. Once identified, much of the work was carried out using LIF in a supersonic jet fluorescence chamber. When desired, the concentration of the water complexes was controlled by splitting off about 15% of the main buffer gas flow, passing it through a reservoir containing water at room temperature (20 °C), and recombining with the main flow before passing through the main sample holder. This technique was also used to produce ABC−$(H_2O)_2$ and ABC−HOD clusters. In the latter case, the water reservoir contained a 50/50 mixture of D_2O/H_2O.

In the case of the ABC−H_2O, ABC−HOD, and one of the B15C−H_2O conformations, more IR transitions than expected were observed in the resonant ion-dip infrared (RIDIR) spectra, leading to the design of the IR−IR−UV hole-burning spectroscopic method, the details of which have been previously described.[19] Essentially it consists of the addition of a second IR hole-burning laser to obtain a modified version of the RIDIRS experiment described earlier.[23] Under conditions in which more than one cluster isomer is suspected of contributing to the UV spectrum at the UV monitor wavelength used, one IR laser can be fixed on a unique transition in the IR, and a second tuned through the spectrum. The ordering and delay of the pulses was set so that IR(1) and IR(2) preceded the UV laser by 1−4 μs and 200 ns, respectively. By using active baseline subtraction in a 5 Hz IR(1), 10 Hz IR(2), 10 Hz UV configuration, we obtain a difference IR spectrum of the species responsible for the infrared absorption probed by IR laser 1.

B. Computational Methods. For this work, we have adopted a strategy similar to that used on the isolated crown ethers (see preceding paper[18]), in which an initial conformational search was carried out using a molecular mechanics force field (MMFs[24−28]) as implemented in Macromodel[29] (10 000 iterations, 10 000 steps, 0.0001 convergence on gradient, 50 kJ/mol energy windows). Since the monohydrated experimental results clearly showed that the only observed structures were those in which both water hydrogens were involved in hydrogen bonds to crown oxygens, the 4100 minima located using the force field were then screened to extract only those structures containing two such water···ether oxygen H-bonds. These 1524 minima having both water hydrogens within 2.5 Å of a crown oxygen were then used to initialize geometry optimizations with the Becke3LYP (B3LYP)[30,31] density functional theory method with the 6-31+G(d) basis set. The first round of optimizations was performed with a default grid and *loose* optimization criteria. The unique low-lying minima (98 below 20 kJ/mol) determined by comparison of electronic energies (tolerance 0.01 kJ/mol) and rotational constants (sum of absolute values of percent differences between isoenergetic structures, 5% tolerance) were then reoptimized using DFT with an *ultrafine* grid and *tight* optimization criteria before DFT harmonic frequencies and single-point second order Möller-Plesset perturbation[32] (MP2) energies were calculated. Both the B3LYP and MP2 calculations were carried out with the GAUSSIAN 03 suite of programs.[33]

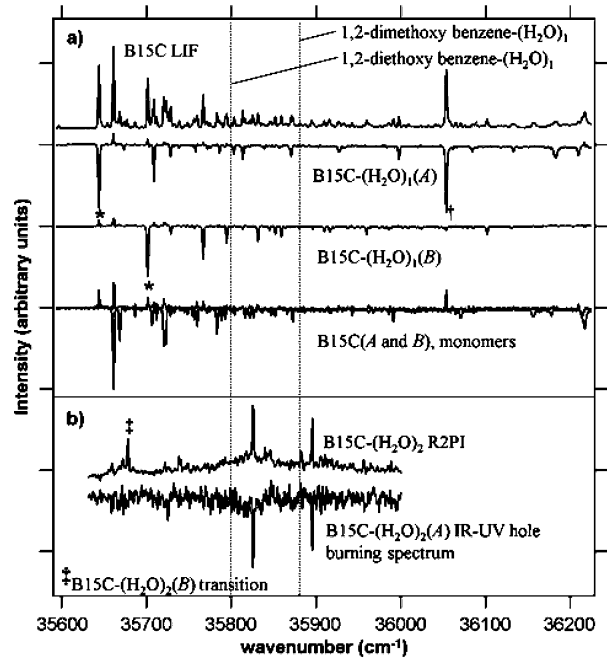

Figure 1. (a) LIF and UV−UV hole-burning spectra of B15C−$(H_2O)_1$ and (b) R2PI and IR−UV hole-burning spectra of B15C−$(H_2O)_2$. Asterisks (*) mark transitions on which the hole-burning laser was fixed in obtaining the indicated UV−UV hole-burning spectra. The dagger (†) marks the transition +409 cm^{-1} above the S_1 origin of B15C−$(H_2O)_1$(A). The double dagger (‡) marks a transition in the B15C−$(H_2O)_2$ R2PI spectrum that did not burn out with B15C−$(H_2O)_2$(A), assigned as the electronic origin of B15C−$(H_2O)_2$(B).

III. Results and Analysis

A. Conformation-Specific Spectroscopy. ***1. UV Spectra.*** The excitation and UVHB spectra of B15C−$(H_2O)_{n=1,2}$ and ABC−$(H_2O)_{n=1,2}$ are presented in Figures 1 and 2, respectively. The initial experiments were carried out on ABC−$(H_2O)_n$ where the congestion present in the spectra with water in the expansion required R2PI scans, shown in Figure 2, to verify the cluster

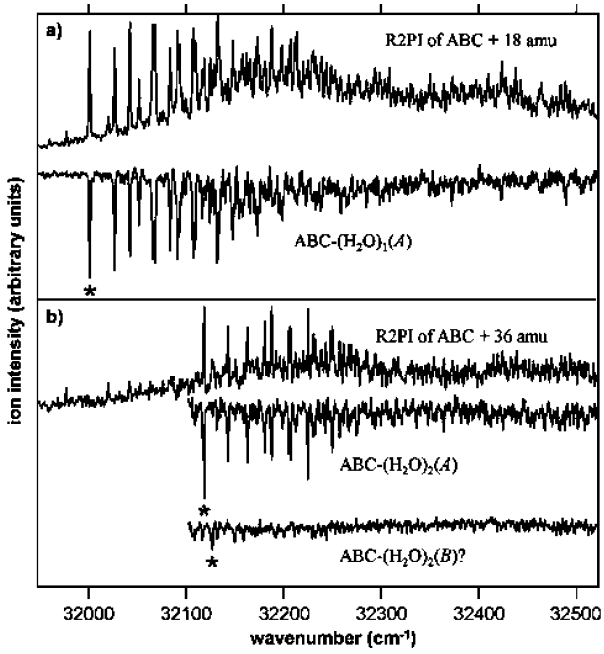

Figure 2. R2PI and UV−UV hole-burning of ABC−$(H_2O)_{n=1,2}$. Asterisks (*) mark transitions on which the hole-burning laser was fixed in obtaining the UV−UV hole-burning spectra.

sizes (mono or dihydrated). The B15C spectra did not suffer this same degree of congestion and the spectrum in the top trace of Figure 1a was recorded using fluorescence detection. R2PI scans (not shown) were used to verify that, in the origin regions, the spectra assigned to B15C−$(H_2O)_1$ arose from masses (268 + 18 amu) corresponding to B15C−$(H_2O)_1$. The R2PI spectrum recorded while monitoring the B15C−$(H_2O)_2^+$ mass channel is shown in Figure 1b.

The UVHB spectra identify two conformations of B15C−$(H_2O)_1$, labeled A and B, recorded by fixing the hole-burning laser on the transitions marked by asterisks in Figure 1a. The UVHB spectra of two monomer conformations with origins in the same region as the water clusters are overlaid in the bottom trace of Figure 1a for comparison with the LIF spectrum in the top trace. For B15C−$(H_2O)_2$, an IR−UV hole-burning spectrum was recorded while hole-burning on a unique IR transition due to conformer A at 3562 cm^{-1}. The transition marked by a dagger did not burn out and was thereby identified as a second conformer of B15C−$(H_2O)_2$. Its RIDIR spectrum (shown in the next section) confirms this assignment.

The UVHB spectrum recorded while monitoring the transition marked by an asterisk in the ABC−$(H_2O)_1^+$ mass channel in Figure 2a accounts for most of the structure in the R2PI spectrum. The corresponding UVHB spectrum in the ABC−$(H_2O)_2^+$ mass channel accounts for all major transitions in this mass channel, and identifies the remaining transitions in ABC−$(H_2O)_1^+$ as transitions due to ABC−$(H_2O)_2$ fragmenting following photoionization into the ABC−$(H_2O)_1^+$ mass channel.

In both B15C and ABC, monomer conformations[18] were found with origins blue-shifted by over 500 and 1000 cm^{-1}, respectively, from the regions shown in Figures 1 and 2. However, no origin transitions due to mono- or dihydrated complexes were discovered near these origins, evidence that the conformational preferences of the isolated crown cycle are quite different from those of the water complexes.

The electronic spectra for all of the B15C−$(H_2O)_n$ complexes (Figure 1) contain very similar vibronic structure and intensity patterns, with the exception of the strong transition in the B15C−(H_2O)(A) conformation 409 cm^{-1} above the origin, discussed in the Supporting Information. The S_0-S_1 origin transitions of B15C−H_2O(A) and (B) are separated from one another by 57 cm^{-1}, appearing at 35 628 and 35 685 cm^{-1}, respectively. This separation is small enough to suggest that the two possess very similar crown ether cycle conformations, at least near the benzene chromophore. If the crown cycle were to assume the same geometry in both conformations, then the two isomeric structures would differ only in the way in which the single water molecule binds to the crown. The positions of the origins are also indicative of an all-planar arrangement of the atoms near the ring, since they are in the same region as origins for monohydrated 1,2-dimethoxybenzene[34] and 1,2-diethoxybenzene (whose positions are marked by dotted lines in Figure 1), and close to the corresponding B15C and ABC monomer origins for such structures (see preceding paper).[18]

The electronic spectra for ABC−$(H_2O)_{n=1,2}$ (Figure 2) are also similar in terms of vibronic activity and intensity patterns, again suggesting similar crown cycle conformations for both near the benzene chromophore. Evidence for a second ABC−$(H_2O)_2$ conformation with UVHB spectrum is shown in the bottom trace of Figure 2. The close proximity of its S_0-S_1 origin to the dominant ABC−$(H_2O)_2$ isomer suggests a minor structural difference between the two. Because the transitions due to this second conformer are so weak, we concentrate on the main ABC−$(H_2O)_2$ complex in what follows.

Compared with the intensities of B15C water complexes, the intensity of the low-frequency vibronic structure is much greater in the ABC water complexes, reflecting a larger geometry change between ground and excited state in ABC−$(H_2O)_n$. One aspect of this geometry change likely involves the amino group, as in aniline it has been hypothesized that the geometry of the amino group changes from pyramidal to planar upon S_0-S_1 excitation.[35] This structural change, which accompanies the $\pi-\pi^*$ transition, may also indirectly be transmitted to the crown structure or crown−water intermolecular vibrations.

2. Infrared Spectra. In the preceding paper that described the B15C and ABC monomers, the only source of XH stretch fundamentals in B15C, the alkyl CH stretches, provided spectral signatures of the crown conformation that paired the conformations present in B15C with their corresponding analogs in ABC.[18] In the H_2O complexes, the OH stretch transitions of H_2O provide additional sensitive probes of the H-bonding environment experienced by the H_2O molecule(s).

Figure 3 presents the alkyl CH stretch spectra for the indicated conformers of the B15C and ABC water clusters. All the spectra were recorded using R2PI detection (RIDIR spectroscopy) except for B15C−$(H_2O)_1$, which use fluorescence-dip infrared spectroscopy (FDIR). All six spectra are marked by intense transitions around 2870 cm^{-1}, with little activity above 2930 cm^{-1}. This observation is in striking contrast to the alkyl CH stretch spectra of the B15C and ABC monomers from Figure 4 of the preceding paper,[18] where sharp transitions above 2930 cm^{-1} were characteristic of blue-shifted CH stretches involved in weak hydrogen bonds to ether oxygens. For these types of CH···O interactions to occur, the crown cycle must buckle in on itself to bring the alkyl groups in one part of the ring into close proximity with the ether oxygens elsewhere on the macrocycle. As a result, we interpret the lack of CH stretch activity on the high-frequency side of the spectrum of the water-containing complexes as indicative of a crown structure that prevents crown methylene group hydrogens from interacting with crown oxygens. The difference between the alkyl CH stretch spectra of the monomers and water complexes is strong

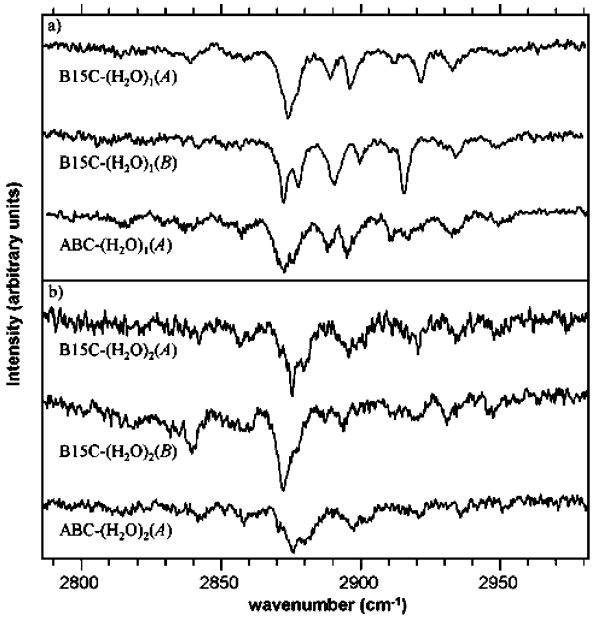

Figure 3. Alkyl CH stretch spectra of B15C$-(H_2O)_n$ and ABC$-(H_2O)_n$ with (a) $n = 1$ and (b) $n = 2$.

evidence that the crown cycle conformation(s) of the water complexes are not the same as those observed in the monomers.

One of the notable aspects of the alkyl CH stretch spectra of Figure 3 is how closely similar the six spectra are to one another. Again, this is in significant contrast to the monomers, where unique signatures for each crown conformation were readily observed. The similarity between ABC$-(H_2O)_1$ and B15C$-(H_2O)_1$(A) is especially notable, implying the crown cycle geometry in the water complex is the same in both molecules. The small differences between all the spectra shown in Figure 3 leads us to initially hypothesize that the crown cycles geometries are the same in all six crown−water complexes. The only difference in these complexes would then be the nature of the water binding site(s).

The RIDIR spectra of the two conformers of B15C$-(H_2O)_1$ and the single ABC$-(H_2O)_1$ conformer in the OH and NH stretch regions are presented in Figure 4a). The positions of both the symmetric stretch (SS) and antisymmetric stretch (AS) fundamentals of H_2O in the complexes are shifted to lower wavenumber by about 90 and 120 cm^{-1}, respectively, from the corresponding frequencies of water monomer (3657 (SS) and 3756 cm^{-1} (AS)).[36] The shift of both fundamentals below 3650 cm^{-1} indicates that both water hydrogens are participating in intermolecular hydrogen bonds. The close similarity between the OH stretch spectra of B15C$-H_2O$ and ABC$-H_2O$ strongly suggests that the water is hydrogen bound to the same crown oxygens in both molecules with no participation by the amino group of ABC in the latter case.

The OH stretch spectra of B15C$-H_2O$ and ABC$-H_2O$ are striking in two respects. First, the splitting between the SS and AS is significantly smaller in the complexes (56, 68, and 68 cm^{-1} for B15C$-H_2O$(B), B15C$-H_2O$(A), and ABC$-H_2O$, respectively) than in free water (99 cm^{-1}).[36] Second, the AS transitions of B15C$-H_2O$(A) and ABC$-H_2O$ are split into a doublet and triplet of transitions, respectively (see insets in Figure 4a).

The OH stretch spectra of the dominant isomer of ABC$-(H_2O)_2$ and B15C$-(H_2O)_2$(A) (Figure 4b) have two nearly equal intensity transitions in the SS region, and a single slightly broadened transition with about twice the intensity in the AS region. If we assume that the doubled intensity in the AS region is due to a partial overlap of the two AS transitions from each H_2O molecule, these spectra are, to a very good approximation, the sum of the B15C$-(H_2O)_1$(A) and -(B) spectra. This observation suggests that the two water molecules in ABC$-(H_2O)_2$ and B15C$-(H_2O)_2$(A) do not H-bond to one another but instead take up two independent double-donor sites to the crown ether.

In contrast, the spectrum of B15C$-(H_2O)_2$(B) is strikingly different, with a free OH stretch transition at 3711 cm^{-1}, and three H-bonded OH stretch fundamentals at 3379, 3504, and 3593 cm^{-1}, the lowest frequency of which is almost 200 cm^{-1} below any of the transitions of the other crown$-(H_2O)_1$ and crown$-(H_2O)_2$ clusters. These results point to a cooperative strengthening of H-bonds, as would occur if a bridging OH···OH···O subunit were present, for instance, in a structure with a water−water H-bond. To connect these spectral features with specific structures, in the next section we will compare the experimental spectra with those predicted by calculations.

The NH stretch frequencies for the ABC$-(H_2O)_{1,2}$ complexes (3400−3500 cm^{-1} region) offer some evidence that the conformation of the crown ether near the ring is planar in both cases. Both the NH symmetric and asymmetric stretch (SS and AS, respectively) frequencies for the water complexes occur within 2 cm^{-1} of those for ABC(C), a conformer assigned to a structure in which the crown is all-planar near the aromatic ring. This close proximity is thus consistent with an all-planar assignment for the water complexes, as long as water complexation to the aromatic oxygens does not shift the NH fundamentals across the phenyl ring. B3LYP frequency calculations bear out this assumption, predicting all of the NH stretch fundamentals for structures containing the crown conformation of B15C$-(H_2O)_1$-(I and II) to be within ~2 cm^{-1} of 3401 and 3492 cm^{-1} for the symmetric and antisymmetric NH_2 stretches, respectively (see, Supporting Information Table S1).

B. Comparison between Experiment and Calculation. ***1. B15C−H₂O and ABC−H₂O.*** Figure 5 shows the double-donor water structures computed for B15C$-H_2O$ within 5.0 kJ/mol of the global minimum at the zero-point corrected (with B3LYP/6-31+G(d) unscaled frequencies) single-point MP2/aug-cc-pVDZ level of theory. The relative energies, TDDFT single-point S_0-S_1 separations, and binding energies for B15C$-(H_2O)_n$ and ABC$-(H_2O)_n$, $n = 1, 2$ are included in Table 1, while the corresponding scaled harmonic OH stretch vibrational frequencies and HOH bending angles are reported in Table 2.

Figure 6a provides a visual comparison of the calculated CH and OH stretch infrared spectra for B15C$-H_2O$ with experiment. On the basis of several pieces of evidence, we assign B15C$-(H_2O)_1$(A) to structure I and B15C$-(H_2O)_1$(B) to structure II. First, of the low-energy structures in Figure 6, only structures I and II have a nominally in-plane structure for the C_β and C_γ atoms on both sides of the aromatic ring, consistent with the TDDFT predictions for the position of the S_0-S_1 energy separations. Second, these structures share the same crown conformation with different binding sites for the water molecule, as we had surmised on the basis of the similarity of the alkyl CH stretch spectra for the two isomers. This crown conformation is one in which the crown is no longer buckled but has opened up to accommodate the binding of water to oxygen sites on opposite sides of the crown.

Furthermore, these double-donor water structures have a calculated OH SS/AS splitting well below that calculated for the water monomer, in keeping with experiment. The results for singly H-bonded structures are not included in Table 2, but

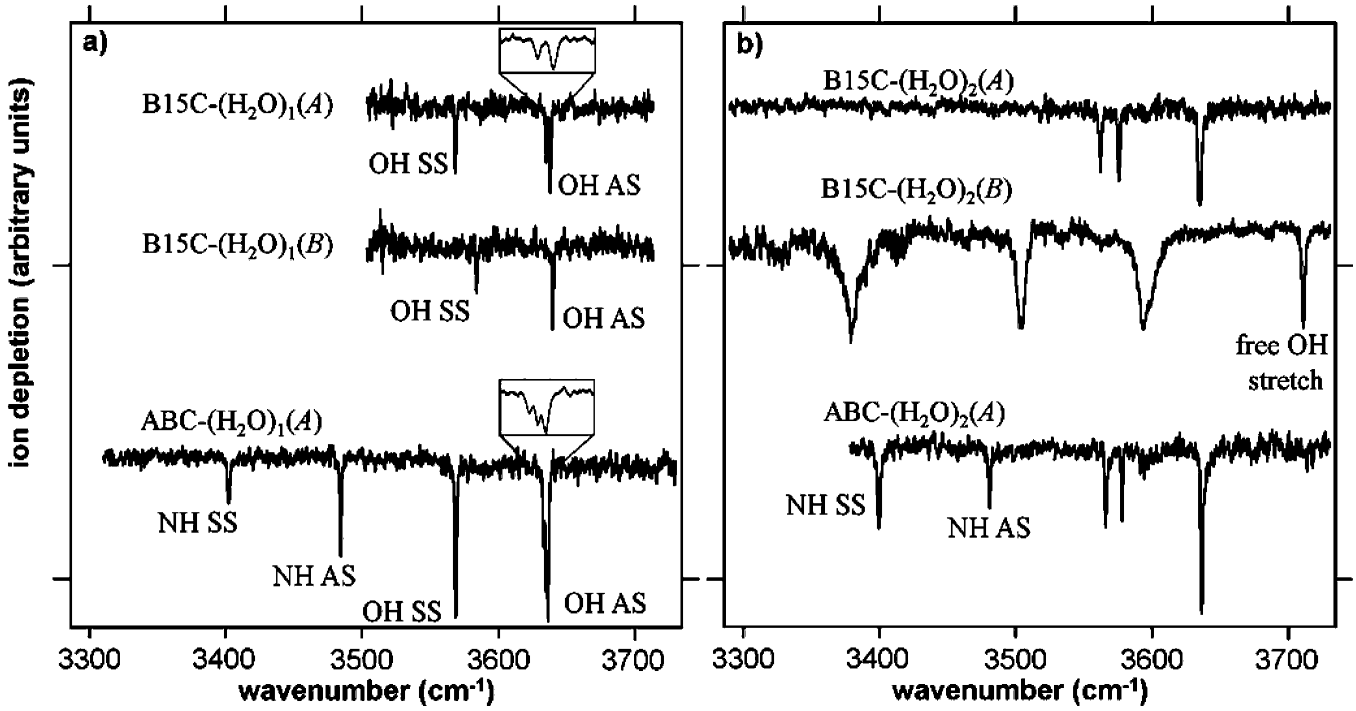

Figure 4. RIDIR spectra in the OH stretch region of B15C−$(H_2O)_n$ and OH/NH stretch regions of ABC−$(H_2O)_n$ for (a) $n = 1$ and (b) $n = 2$. Insets in part (a) show close-up views of the doublet and triplet observed in OH AS of B15C−$(H_2O)_1$(A) and ABC−$(H_2O)_1$(A), respectively.

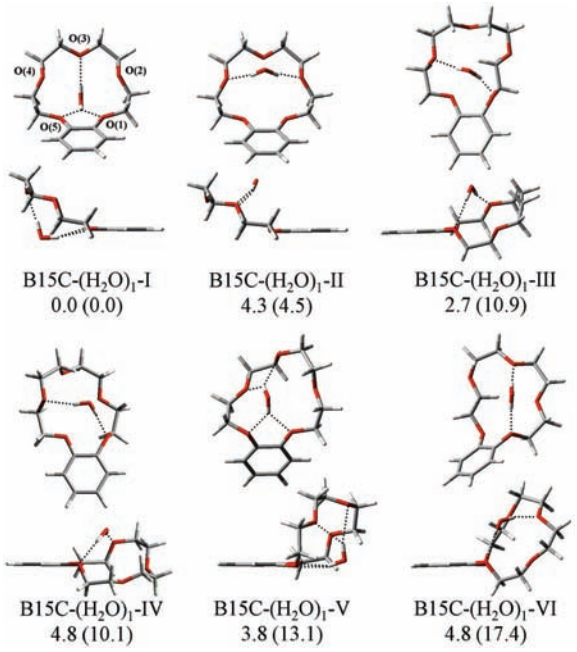

Figure 5. Calculated low-energy structures of B15C−$(H_2O)_1$. Two views, front and side, are given for each structure. Single-point, zero-point corrected MP2/aug-cc-pVDZ energies are given, with ZPC B3LYP/6-31+G(d) energies in parentheses. Dashed lines indicate hydrogen bonds. Energy units are kJ/mol.

these consistently show free OH stretch transitions near 3720 cm^{-1} and H-bonded OH stretches varying from 3470 to 3585 cm^{-1}, producing splittings of 135−250 cm^{-1} or more. The assignment of B15C−$(H_2O)_1$(A) to structure I and B15C−$(H_2O)_1$(B) to II is also consistent with the larger splitting calculated for the former over the latter.

Both of these structures are at or near the global minimum at both the DFT and MP2 level, strengthening the assignment. The other low-energy structures have "buckled" crown geometries that lead to interactions between different parts of the crown cycle as well as more interaction between the crown cycle and water. While much of this interaction may be stabilizing, it is likely that the MP2 method is overestimating the stabilizing effects of the dispersive interactions (likely due to intramolecular basis set superposition errors)[37] and thus the stability of these conformations relative to B15C-I and B15C-II. For comparison, the DFT energies calculated with the M05-2X functional,[38] designed to better describe dispersive interactions, are given in Table 1 and give support to this hypothesis.

Additionally, as shown in Figure 6a, the observed alkyl CH stretch and water OH stretch spectra of B15C−$(H_2O)_1$ A and B are fit reasonably well by the calculated spectra for I and II. In particular, the symmetric structure, which possesses C_s symmetry, does not allow crown methylene groups to form hydrogen bonds with crown oxygens and thus almost all of the CH stretch transitions fall below 2930 cm^{-1}.

Since the 68 cm^{-1} splitting between the SS and AS OH stretch fundamentals of the sole observed isomer of ABC−$(H_2O)_1$ is identical to that found in B15C−$(H_2O)_1$ A, we also associate the only confirmed conformer of ABC−$(H_2O)_1$ with structure I, in which the water is bound to the benzo oxygens.

2. B15C−$(H_2O)_2$ and ABC−$(H_2O)_2$. Figure 7 shows three low-energy structures calculated for B15C−$(H_2O)_2$. Structure I has the two water molecules occupying the two lowest energy binding sites in the $n = 1$ complex, assigned previously to conformers *A* and *B* of B15C−$(H_2O)_1$, while structures II and III have the second water molecule donating a single H-bond to the double-donor water molecule in either of these two positions.

Figure 6b compares the experimental and calculated IR spectra for B15C−$(H_2O)_2$. The calculated spectra confirm the structural deductions made on the basis of a comparison of the $n = 2$ spectra with those for $n = 1$. The calculated spectrum of B15C−$(H_2O)_2$-I is very nearly the sum of the spectra due to the $n = 1$ I and II structures, matching experiment closely. We therefore assign B15C−$(H_2O)_2$ A (and ABC−$(H_2O)_2$, by

TABLE 1: Conformational Assignments and Experimental and Computational Summary for B15C−$(H_2O)_n$ and ABC−$(H_2O)_n$ (n = 1, 2), Including Electronic S_0−S_1 Origins, Scaled[a] TDDFT B3LYP/6-31+G(d) Results, Relative Energies,[b] and Binding Energies[c,d]

			S_0−S_1		relative energy (kJ/mol)[b]			binding energy (kJ/mol)[c]	
molecule	structure	assignment	origin	TDDFT[a]	B3LYP	MP2	M05-2X	B3LYP	MP2
B15C−$(H_2O)_1$	I	A	35628	35539	0.00	0.00	0.00	36.64	39.22
	II	B	35685	35505	4.48	3.99	6.37	32.16	35.23
	III			36341	10.87	3.07	6.35	29.71	30.85
	IV			36103	10.05	4.53	8.29	32.51	33.29
	V			35029	13.14	2.66	9.53	34.11	36.71
	VI			36996	17.40	4.56	11.04	25.73	28.21
B15C−$(HOD)_1$	I-a			35539	0.00	0.00		38.00	40.58
	I-t			35539	0.24	0.24		37.76	40.34
	II			35505	4.89	4.40		33.11	36.18
B15C−$(H_2O)_2$	I	A	35813	35736	4.25	0.42	0.00	30.08	50.46
	II	B	35665	35565	0.00	0.00	10.07	34.33	50.88
	III			35527	3.56	0.36	14.40	30.77	54.79
ABC−$(H_2O)_1$	I-dn	A	31998	32203	0.16	0.20		37.29	39.68
	I-up			32281	0.00	0.00		37.50	39.89
	II-dn			32160	4.50	4.11		32.95	35.78
	II-up			32192	5.23	4.86		32.27	35.04
ABC−$(HOD)_1$	I-dn-a	A	31998	32203	0.16	0.20		38.64	41.04
	I-up-a			32281	0.00	0.00		38.85	41.25
	I-dn-t	B	31998	32203	0.20	0.44		38.60	40.80
	I-up-t			32281	0.24	0.24		38.61	41.01
	II-dn-t			32160	4.61	4.22		34.19	37.02
	II-up-t			32192	5.35	4.98		33.51	36.27
	II-dn-a			32160	4.61	4.21		34.20	37.03
	II-up-a			32192	5.34	4.97		33.52	36.28
ABC−$(H_2O)_2$	I/II-dn	A	32115	32296					
	I/II-up			32358					

[a] Excited state 1 scaled by 0.896 12 for B15C complexes. ABC complexes are predicted excited state 2 scaled by 0.898 91. See preceding paper[18] for explanation of use of predicted excited state 2 instead of excited state 1. [b] Zero-point corrected energies using unscaled B3LYP frequencies. MP2 energies are basis set superposition error corrected via counterpoise correction except for dihydrated complexes. [c] Binding energy = $E_{ZPC}(n = 1,2) - E_{ZPC}(n = 0,1) - E_{ZPC}$(water monomer). [d] Structure names suffixed with "a" or "t" refer to the orientation of the HOD D atom toward the O(3) crown oxygen or toward the benzene ring, respectively. Structures containing "dn" or "up" refer to the orientation of amino group lone pairs as trans or cis, respectively, to the O(3) oxygen.

analogy) to structure I, in which the two water molecules simultaneously occupy the binding sites of B15C−H_2O(A) and B15C−H_2O(B). The stick spectra in the CH stretch region for the unassigned structures are included in the Supporting Information (Figure S1). As for the monohydrated conformations, these spectra confirm the same open crown structure deduced for the $n = 1$ complexes.

The deduced structure (structure B15C−$(H_2O)_2$-I), is striking, with the two water molecules occupying positions on opposite sides of the crown, perpendicular to each other. The crown itself is curved out of the plane of the phenyl ring, placing two crown oxygens in symmetric positions pointing their lone pairs into the interior curved surface that can accept a water molecule oriented perpendicular to the C_s plane of the crown. The other water molecule occupies a site on the opposite side of the crown, on the back side of the curved surface, parallel to the C_s plane, forming one normal OH···O and one three-center H-bond with the two aromatic ring oxygens.

The second dihydrated B15C complex, B15C−$(H_2O)_2$(B), has an alkyl CH stretch spectrum very similar to those of the previously discussed conformations. However, the OH stretch spectrum for this conformation contains three very broad transitions below 3600 cm^{-1} and a relatively narrow transition above 3700 cm^{-1}, standing in stark contrast to the spectra for any of the other $n = 1$ or $n = 2$ complexes. The transition at 3711 cm^{-1} indicates that one of the water hydrogens is not involved in any interaction with either crown oxygens or the oxygen of the other bound water. The three broad transitions reflect a structure in which the three other water hydrogens are involved in hydrogen bonds to crown oxygens and/or water oxygens. Given the preference for the two positions taken up by the water molecules in B15C−H_2O(A,B) and B15C−$(H_2O)_2$(A), structures for B15C−$(H_2O)_2$(B) were formed in which the second water binds to a structure in which the first water takes up one of these positions. Two optimized candidates are presented in Figure 7b,c (structures II and III). Figure 6b and Table 2 compare the RIDIR spectrum of B15C−$(H_2O)_2$(B) with those calculated for these two structures. Both structures II and III fit the qualitative pattern of OH stretch transitions well, confirming a water dimer structure as responsible for the observed spectrum of conformer B. We cannot distinguish with certainty between structures II and III. However, the scaled frequencies of structure II match particularly well for two of the four OH stretches, and the splitting between the transitions assigned to the SS and AS stretch of the doubly hydrogen bound first water is also predicted with good accuracy. This splitting is close to that in B15C−$(H_2O)_1$(A), which has the water bound to the crown in the same binding site as in structure II.

On the basis of the calculated form of the normal modes, the transition at 3379 cm^{-1} can be assigned to the H-bonded OH stretch fundamental of the single donor water. Its frequency is 161 cm^{-1} lower than in the free water dimer (3530 cm^{-1}),[39] reflecting strong cooperative strengthening of this H-bond by the fact that the acceptor water is doubly bound to the crown. This frequency lowering was also noted by Kusaka et al. in their study of DB18C6−$(H_2O)_2$, where this structure was the only one observed.[11] Due to the small ion signal, RIDIR scans

TABLE 2: Conformational Assignments and Experimental (Exp) and Computational (Cal) Summary for B15C−$(H_2O)_n$ and ABC−$(H_2O)_n$ (n = 1, 2), Including Scaled B3LYP/6-31+G(d) Harmonic Frequencies for Antisymmetric and Symmetric Stretching H_2O Modes and HOH Bond Angles

			SS OH (cm^{-1})		AS OH (cm^{-1})		splitting (cm^{-1})		
molecule		assign-ment	exp	cal	exp	cal	exp	cal	H−O−H bond angle (deg)
water			3657	3635	3756	3756	99	121	105.488
DMB−$(H_2O)_1$			3586	3583	3725	3734	139	151	104.92
B15C−$(H_2O)_1$	I	A	3569	3562	3637	3660	68	99	103.117
	II	B	3584	3574	3640	3650	56	76	103.011
	III			3571		3653		82	103.498
	IV			3560		3637		77	103.223
	V			3595		3673		78	102.07
	VI			3565		3649		83	103.945
B15C−$(H_2O)_2$	I	A	3562, 3576	3561, 3571	3635, 3635	3661, 3650	73, 59	100, 79	103.5, 103.4
	II	B	3504, 3379[a]	3503, 3320[a]	3618, 3711[b]	3623, 3714[b]	114, 332	120, 394	103.5, 106.1[c]
	III			3298,[a] 3528		3713,[b] 3584		415, 56	103.3, 106.1[c]
ABC−$(H_2O)_1$	I-I	A	3567	3563	3635	3658	68	95	103.129
	I-II			3563		3658		95	103.123
	II-I			3573		3649		76	102.986
	II-II			3574		3650		76	103.015
ABC−(HDO)	I-dn-a	A	2633	2604	3620	3639	987	1036	103.129
	I-up-a			2603		3639		1036	103.123
	I-dn-t	B	2660	2643	3583	3584	923	940	103.129
	I-up-t			2643		3583		940	103.123
	II-dn-t			2625		3611		986	102.986
	II-up-t			2626		3611		985	103.015
	II-dn-a			2629		3623		994	102.986
	II-up-a			2623		3615		992	103.015
ABC−$(H_2O)_2$	I/II-dn	A	3577, 3566	3580, 3569	3636, 3636	3669, 3658	70, 59	100, 78	103.5, 103.3
	I/II-up			3580, 3570		3669, 3658		99, 78	103.5, 103.3

[a] Bound OH oscillator of water hydrogen bonded to first water bound to the crown ether. [b] Free OH oscillator of water hydrogen bonded to first water bound to the crown ether. [c] HOH bond angle of water not bound directly to crown ether but to first bound water.

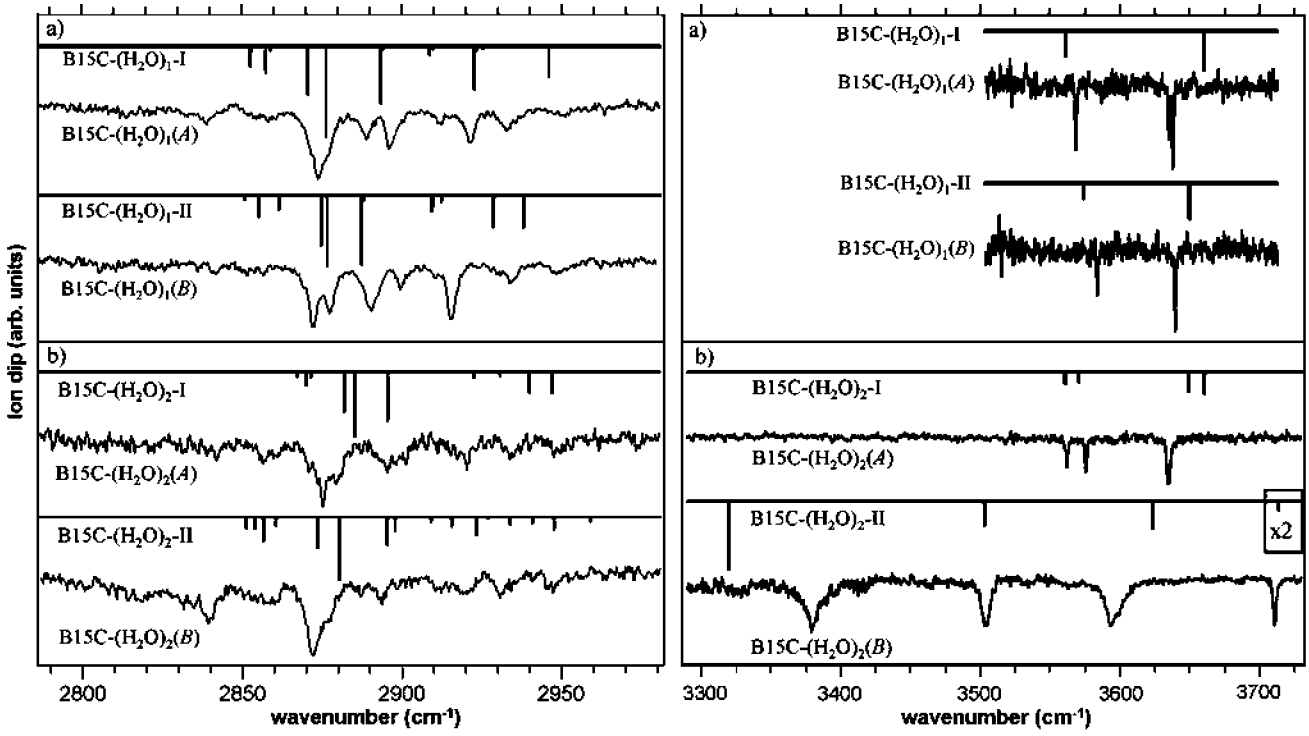

Figure 6. Comparison of experimental and predicted alkyl CH and OH stretch spectra calculated at the B3LYP/6-31+G(d) level of theory. The calculated alkyl CH and OH stretch vibrational frequencies were scaled by 0.958 and 0.975, respectively. The best-fit calculated spectra are shown immediately above each of the experimental spectra.

of this conformer were recorded at high-IR power conditions which saturated the transitions. Therefore, the calculated greater intensity of this lowest frequency OH stretch fundamental is obscured in the experimental spectrum.

C. Further Probes of Water's Binding to the Crown. The two structures just deduced in section B1 for the B15C−H_2O complex have the water molecule taking up two complementary binding sites on the same open crown structure, one parallel to

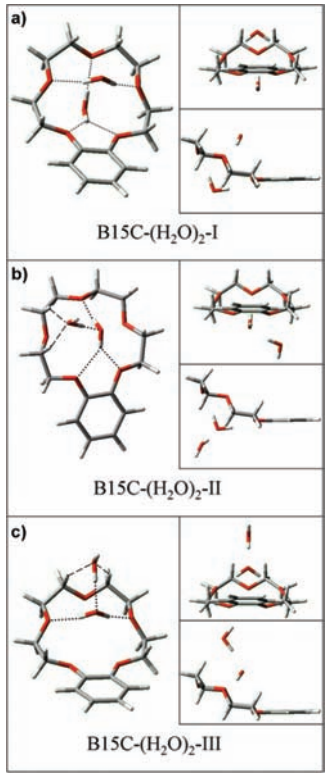

Figure 7. Low-energy B15C−$(H_2O)_2$ structures optimized at the B3LYP/6-31+G(d) level of theory. Dotted lines indicate OH···O hydrogen bonds while dashed lines indicate CH···O hydrogen bonds.

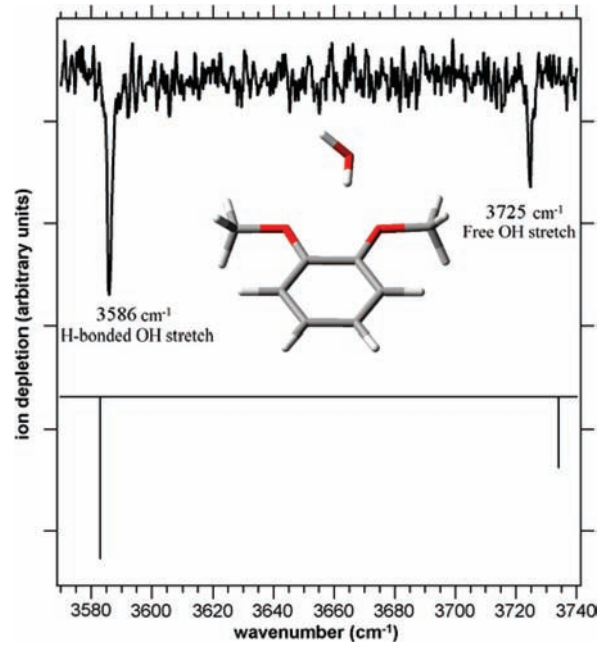

Figure 8. RIDIR spectrum in OH stretch region of DMB−H_2O compared with OH stretch vibrational frequencies and infrared intensities calculated at the DFT B3LYP/6-31+G(d) level of theory. The optimized structure for DMB−H_2O is shown as an inset.

the phenyl ring (Figure 5, structure I) and the other perpendicular to it (Figure 5, structure II). Taken together, structures I and II use all five of the crown ether oxygens in their binding, with structure I incorporating a three-center H-bond with the two benzo oxygens and the other OH binding to a single oxygen atom on the opposite side of the crown. This structure is the only conformation observed in ABC−H_2O. Structure II has two nearly identical H-bonds to the remaining two crown ether oxygens.

In seeking a better understanding of each of these binding sites on the crown, we have carried out two additional experiments. In the first, we remove the rest of the crown in studying the 1,2-dimethoxybenzene−H_2O complex, leaving only the benzo-oxygen sites for water binding. In the other, we study the ABC−HOD isotopomer, with its spectroscopically distinguishable OH and OD bonds for binding to the crown. This complex was used to illustrate the IR-IR−UV method introduced previously.[19] Here, we focus on the insight these spectra bring to the binding of water to the crown ether.

1. 1,2-Dimethoxybenzene−H_2O Complex. Figure 8 shows the OH stretch RIDIR spectrum of the DMB−H_2O complex. The two OH stretch fundamentals indicate the presence of a single OH···O H-bond in the complex, with one H-bonded OH stretch at 3586 cm^{-1} and a second weaker intensity OH stretch at 3724 cm^{-1}, a value typical for a free OH stretch.[36] The inset of Figure 8 shows the optimized structure for DMB−H_2O at the DFT B3LYP/6-31+G(d) level of theory. As in B15C−H_2O(A), the calculations predict the presence of a three-center H-bond in DMB−H_2O in which the bound OH group points midway between the two benzo oxygen atoms. The calculated OH stretch vibrational frequencies and infrared intensities are also shown. The H-bonded OH stretch fundamental in DMB−H_2O at 3586 cm^{-1} appears close to the symmetric OH stretch in B15C−H_2O(A) (SS at 3569 cm^{-1}). However, according to the calculations, the two OH stretch fundamentals in DMB−H_2O are primarily local mode OH stretch vibrations due to the free and H-bonded OH groups in the complex, with an experimental splitting between them of 139 cm^{-1}, almost exactly twice what the splitting is between SS and AS of H_2O in B15C−H_2O.

The spectrum of Figure 8 requires a refinement of the structure deduced from high-resolution ultraviolet spectroscopy of the DMB−H_2O complex by Yi et al.[34] A full consideration of these structural implications will be taken up elsewhere.[40] For our purposes here, it is sufficient to note that in the structure deduced by Yi et al.,[34] the two OH groups were surmised to point equivalently above and below the plane of the aromatic ring.[34] While the vibrationally averaged geometry may have two equivalent OH groups, the potential energy surface in which the water molecule moves has two distinct minima in which a single OH group is pointed in toward the DMB oxygens, forming a single H-bond.[34]

2. ABC−HOD Complex. Using an isotopic mixture of water in the expansion, ABC−HOD complexes were formed and studied by R2PI and RIDIR spectroscopy. The bottom traces of Figure 9 show the RIDIR spectrum of the ABC−$(HOD)_1$ complex in the OD stretch (left) and OH stretch (right) regions. In the OH stretch region, two of the transitions (marked by daggers) arise from the ^{13}C isotope of ABC−$(H_2O)_1$, which has the same mass and an S_0-S_1 origin transition that partially overlaps that of ABC−HOD. However, even after these transitions were removed from consideration, two OD and two OH stretch transitions were observed, where only one of each was expected. In previous cases where RIDIR or FDIR spectra showed extra transitions, IR−UV hole-burning could be used to record the UV spectrum of the conformation responsible for the extra transition(s). Typically, these spectra would uncover UV transitions from each conformation which were not overlapped with one another. These could subsequently be used to record "uncontaminated" RIDIR or FDIR scans. In the present

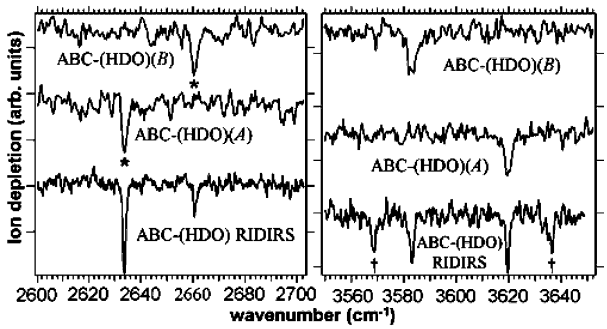

Figure 9. RIDIR and IR−IR−UV hole-burning spectra of ABC−$(HDO)_1$. IR hole-burning laser transitions are marked by asterisks. OH stretch transitions arising from the ^{13}C isotope of ABC−$(H_2O)_1$ (with the same mass as ABC−HOD) are marked by daggers (†).

case, however, the IR−UV hole-burning scans were essentially identical to one another.[19]

In this circumstance, IR−IR−UV hole-burning[19] was used to prove that the two OD and two OH stretch transitions arose from two unique ground state levels due to two different conformations of ABC−HOD. These spectra, recorded with the first IR laser fixed on the transition indicated with an asterisk, are shown in the top two traces of Figure 9. The lower frequency OD stretch fundamental is correlated with the higher frequency OH stretch transition and vice versa. We surmise on this basis that the OH···O and OD···O H-bonds in ABC−HOD involve distinguishable acceptor sites (one stronger and one weaker), with the expansion forming the ABC−HOD complex with the OD bond in either position. This observation strongly suggests that the HOD molecule in ABC−HOD is oriented as in B15C-I (with one H-bond bifurcating the aromatic oxygens and one to an alkyl ether oxygen, Figure 5) rather than B15C-II (involving two nearly equivalent alkyl ether oxygen sites), since there is a larger difference between binding sites in structure I. The computational results support this assignment (Table 2). In the discussion section, the data from these two conformers of ABC−HOD are used to determine quantitatively the frequency shifts produced by uncoupled OH/OD bonds binding to each of the four sites in the crown.

We have also carried out an analogous study of the unusual multiplet structures observed in the AS transitions of B15C−H_2O(A) and ABC−H_2O(A). IR−IR−UV hole-burning scans described in detail in the Supporting Information prove that these multiplets all share the same ground state, pointing to Fermi resonance as the source of the splittings. A 3:1 Fermi resonance with the benzo C−O stretch modes was identified as the likely source, shifted out of resonance in the local mode OH/OD stretch transitions in ABC−HOD.

IV. Discussion

A. Structures and Conformational Preferences of Crown−Water Complexes. The spectroscopic analysis described above has led to assignments for the observed structures of benzo-15-crown-5 and 4′-aminobenzo-15-crown-5 ether complexes with one or two water molecules. In all cases, water acts as a double donor to two or more crown ether oxygen sites, stabilizing the complexes through two intermolecular hydrogen bonds. In B15C−H_2O, the global minimum structure (Figure 5, structure I) has the water molecule aligned along the symmetry plane that bisects the phenyl ring, with the analogous structure in ABC also the global minimum. In ABC, this structure was the only conformer observed while in B15C, transitions assigned to structure I were the most intense in the electronic spectrum. The structure contained a typical two-center hydrogen bond of the "outside" OH group with the crown oxygen opposite the phenyl ring and a second three-center hydrogen bond in which the "interior" water hydrogen is directed toward a point midway between the two aromatic ether oxygens. The distance between the two aromatic crown oxygens is 2.6 Å compared with a distance of about 2.9 Å between adjacent alkyl ether oxygens. This smaller distance, when combined with the preference for an in-plane geometry of both C_β carbons, presents an electron rich region between the two oxygens that forms the best acceptor site in the crown cycle. The odd number of crown oxygens (5) places a single oxygen on the opposite side of the crown cycle, making it well-positioned to act as a second acceptor site.

The three-center H-bond in these complexes is similar to that formed in 1,2-dimethoxybenzene−H_2O (Figure 8). However, in that case, water's oxygen atom was determined to be in the plane of the aromatic ring,[34] while here (Figure 5), the calculated position for the water molecule is pushed out-of-plane to accommodate a second H-bond to the outer oxygen. Finally, according to the calculations, in ABC−H_2O, the asymmetry induced by the amino group causes the water hydrogen involved in the 3-center H-bond to point more toward the aromatic crown oxygen para to the amino group.

The minor monohydrated B15C complex (B15C−$(H_2O)_1$(B)) has the water molecule bound on the opposite side of the crown cycle, on the "interior" of the curved crown surface (Figure 5, B15C−$(H_2O)_1$-II), and perpendicular to the C_s plane of symmetry of the crown. The water again acts a double donor in this isomer, here forming two equivalent OH···O H-bonds with the two oxygens not used in B15C−H_2O(*A*).

In B15C−$(H_2O)_2$(A) and ABC−$(H_2O)_2$, the two water molecules take up the same two positions occupied in B15C−$(H_2O)_1$ A and B, with one parallel and one perpendicular to the plane of symmetry present in the crown (Figure 7, structure I). This double-water structure shares the same open crown conformation as the single water structures.

One of the most striking aspects of the results reported here is that the crown ether conformation associated with the water complexes is not among those observed in the crown ether monomer conformations (see preceding paper[18]). The uncomplexed crown ether assumes more compact, "buckled" crown structures in which one or more of the outer segments folds back in toward the interior of the cycle such that the shortest across cycle distance is typically ≈4 Å as opposed to the ≈5 Å distance of the conformation formed upon complexation to water. This collapsing of the crown structure maximizes the stabilizing attractive interactions between different segments of the macrocycle. In the absence of water complexation, the open crown conformation is 3.5 kJ/mol above the global minimum at the B3LYP/6-31+G(d) level, 15.0 kJ/mol at the single-point MP2/aug-cc-pVDZ level and 14.9 kJ/mol at the single-point M05-2X/6-31+G(d) level of theory. The higher energy of this structure places it above several lower energy monomer conformers into which the molecule can isomerize during collisional cooling in the expansion.

Thus, complexation of a single water molecule has completely shifted the 15-crown-5 conformational preference from the distribution of "buckled" structures to a single, more open structure capable of receiving the first and second water molecules with maximum effect. We surmise on this basis, then, that the 15-crown-5 pocket has a size well-suited to double-donor binding by a single water but stretches the crown to its

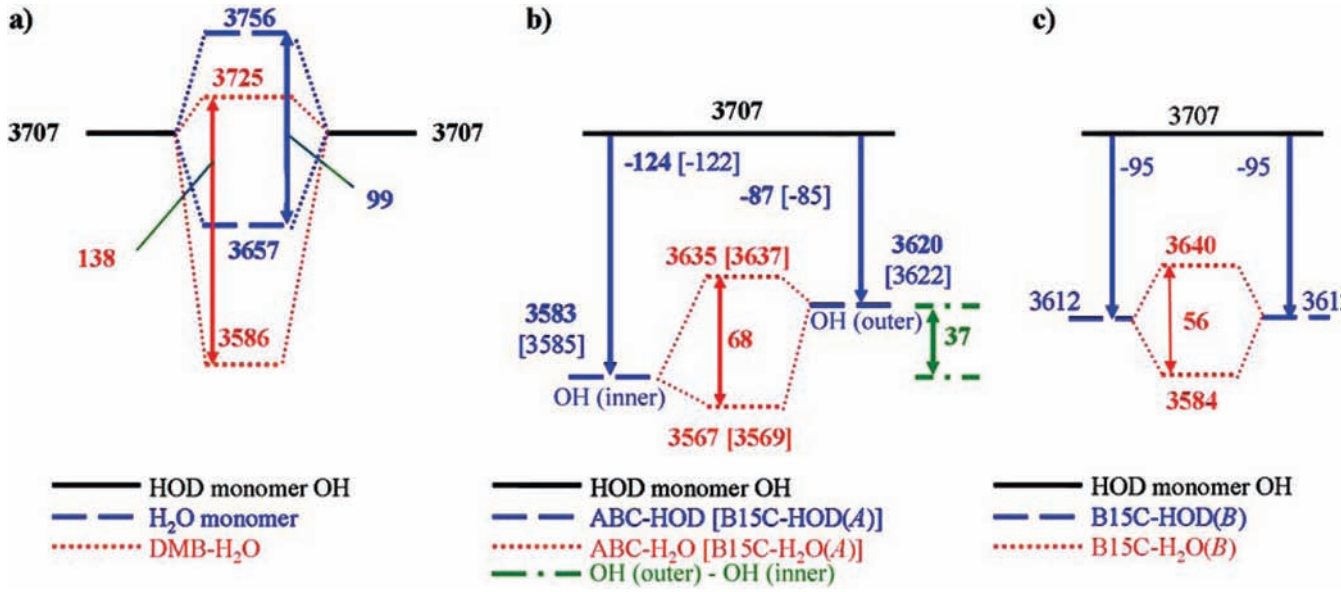

Figure 10. Energy level diagrams for splittings observed between AS and SS OH fundamentals of the water complexes. H_2O and HOD monomer frequencies are from ref 36. (a) Comparison of H_2O monomer (3657, 3756 cm^{-1}, SS/AS split by 99 cm^{-1}) and HOD monomer (3707 cm^{-1}, local mode) with that in DMB−H_2O (3725 cm^{-1} free OH, 3586 cm^{-1} H-bonded OH), with a splitting of 139 cm^{-1}. (b) In ABC−HOD, HOD can be oriented with OH H-bonded to two distinct binding sites on the crown (inner and outer) with different binding strengths (leading to shifts of −124 and −87 cm^{-1}, respectively). The 37 cm^{-1} difference is deduced from the positions of the uncoupled OH stretch fundamentals for these two sites in the two isomers of the ABC−HOD complex, arising from unequal force constants. The remaining 31 cm^{-1} splitting in ABC−H_2O and B15C−H_2O is due to a combination of kinetic and potential coupling. (c) In B15C−HOD(B), the two binding sites are equivalent, with the uncoupled OH levels midway between the observed OH stretch modes and the 56 cm^{-1} splitting between the two observed fundamentals in B15C−H_2O(B) due entirely to kinetic and off-diagonal potential coupling between the two OH groups.

most open structure in so doing. Furthermore, the calculated position of the water molecule in B15C−$(H_2O)_1$(A) (Figure 5, structure I) somewhat out of the aromatic ring plane is computational evidence that a single water molecule just overfills the most open binding pocket in 15-crown-5. That this same open crown structure also competitively binds a water molecule using the other two ether oxygens on the opposite side of the macrocycle speaks to near-ideal fit between a single water molecule and the 15-crown-5 binding pocket approaching either face of the cycle. In comparison, the slightly larger 18-crown-6 counterpart studied by Kusaka et al. may not need to undergo the same structural rearrangement to accommodate the water molecule.[10,11]

Given this near-ideal fit, it is not surprising that the dominant structure for B15C−$(H_2O)_2$ and ABC−$(H_2O)_2$ is an "independent site" structure in which both faces of the open crown ring are occupied. This structure uses all five of the ether oxygens as acceptor sites. Given their inherent stability, these solvent-bound structures may be important in room temperature solution as well. It is these crown-bound water molecules which must be displaced by a cation in forming the well-known cation-crown complexes that play such an important role in solution.

This responsiveness of the cycle to its environment is a hallmark of the crown ethers. The potential energy surfaces of crown ethers are characterized by many low-lying minima,[41−44] a testament to the conformational flexibility inherent in the crown. However, the strong binding sites present in the crown can shift this equilibrium distribution markedly in response to particular binding partners. In this case, a single water molecule has sufficient binding capacity to splay open the crown to maximize the strength of water−crown binding. A second water can bind to the opposite side of the crown, taking up the two remaining ether oxygen sites forming a stable, beautifully symmetric structure (Figure 7a).

In close competition with this "independent site" water−crown binding of structure I (Figure 7a) is a second structure for B15C−$(H_2O)_2$ in which the second water forms a water dimer, with the first water taking up the parallel double-donor binding site, with the second acting as donor to the first. As Kusaka et al. have noted, this structure benefits from cooperative strengthening of the water(1)−crown H-bonds that shifts their frequencies by 40−80 cm^{-1} relative to their positions in the $n = 1$ complex.

B. Spectroscopic Signatures of the Water−Crown Binding. The structural assignments for the crown water complexes resulted from the size and conformation-selective UV and IR spectra of B15C−$(H_2O)_n$, ABC−$(H_2O)_n$, and ABC−HOD ($n = 1$ or 2). Armed with these assignments, we return to the spectra themselves to highlight the unusual effects of the crown on the spectral properties of the water molecules and visa versa. The analysis that follows determines the frequency shifts associated with uncoupled OH groups H-bonding to each of the unique oxygen sites on the crown.

When water binds to the crown as a double donor to the crown oxygens, it produces two characteristic effects on the OH stretch fundamentals of the bound water molecule: (i) a large shift to lower frequency in both OH stretch transitions and (ii) simultaneously decreasing the splitting between them from their corresponding values in the water monomer.

The spectrum of DMB−H_2O in Figure 8 reminds us of the more common circumstance in which a H_2O molecule forms a single H-bond between one of its OH groups and an acceptor site on its binding partner. Figure 10a summarizes this result in an energy level diagram that compares the OH stretch fundamentals of H_2O monomer to those in DMB−H_2O. When H_2O acts as a single donor, the H-bonded OH stretch decreased in frequency, while the free OH moves toward a frequency just above the uncoupled OH. This produces a splitting between the two OH stretch fundamentals that is much greater than the 99 cm^{-1} splitting in the monomer. In DMB−H_2O, this splitting is 139 cm^{-1}.

The corresponding energy level diagrams for ABC−$(H_2O)_1$, the two isomers of ABC−HOD, and the two isomers of B15C−$(H_2O)_1$ are incorporated into Figure 10b,c. In B15C−H_2O(A) and ABC−$(H_2O)_1$, the splitting between the two OH stretch fundamentals is 68 cm^{-1} and in B15C−H_2O(B) it is 56 cm^{-1}, reductions by some 30−50% from the splitting in the water monomer (99 cm^{-1}).[36] The calculated structures also show this decreased splitting relative to the water monomer (Table 2). Although the calculated frequency splittings are not quantitatively correct, qualitatively the correct trends are captured, with the calculated splitting for B15C−H_2O(A) larger than that for isomer B, as observed experimentally.

The energy level diagrams in Figure 10 use the uncoupled OH stretch transitions in HOD monomer and the two isomers of the ABC−HOD complex as starting points for understanding the observed wavenumber positions and splittings in ABC−$(H_2O)_1$ and the two isomers of B15C−$(H_2O)_1$. That the OH stretch in HOD monomer is essentially uncoupled from its partner O−D bond is apparent in that the OH fundamental in HOD (3707 cm^{-1}) is precisely midway between the SS (3657 cm^{-1}) and AS (3756 cm^{-1}) fundamentals of H_2O.[36] On this basis, we deduce that the observed OH stretch transitions in the two isomers of ABC−HOD, 3583 cm^{-1} for OH(inner) and 3620 cm^{-1} for OH(outer), are the uncoupled wavenumber positions of the OH fundamentals associated with the inner H-bond to the benzo-oxygens and the outer H-bond to the crown oxygen opposite it (denoted as O(3) in Figure 5), respectively. Since the wavenumber positions in B15C−H_2O(A) are virtually identical to those in ABC−H_2O, similar values are surmised for this structure as well. Using the OH stretch of HOD monomer as reference, this indicates that the three-center OH···benzo oxygen H-bond produces a wavenumber shift of −124 cm^{-1}, while that for the OH···O(3) crown is −87 cm^{-1}.

Similar arguments can be made for the B15C−H_2O(B) isomer. In this case, the two OH···O H-bonds are to the equivalent O(2) and O(4) crown ether oxygen sites. For this reason, the two OH stretch modes in isomer B are calculated to be fully delocalized over both OH groups, producing SS and AS modes with equal amplitude motion of the two OH bonds. Thus, the uncoupled OH stretch positions would occur midway between the observed 3584 and 3640 cm^{-1} SS and AS transitions, at 3612 cm^{-1}. In the absence of coupling, these two OH fundamentals are shifted −95 cm^{-1} from the OH stretch of HOD monomer, a value intermediate between the shifts deduced for the two crown sites present in the A isomer.

These simple arguments provide a clear picture of the H-bonding present in the two isomers of B15C−$(H_2O)_1$. In isomer A, the electron-rich pocket created by the two benzo oxygens is the best acceptor site for a water OH group. Not surprisingly, the B15C−$(H_2O)_1$ isomer that dominates the spectrum (isomer A) uses this site as one of its two sites in binding to the crown. Its uncoupled wavenumber position in B15C−H_2O(*A*) (3585 cm^{-1}) is close to that in DMB−H_2O (3586 cm^{-1}). At the same time, the second OH group in B15C−H_2O(A) forms a H-bond with the crown oxygen across the macrocycle (O(3)) but in so doing must compromise the strength of this H-bond to some degree to maximize its interaction with the benzo oxygens. As a result, the wavenumber position of the uncoupled OH to O(3) is 3622 cm^{-1}, about 10 cm^{-1} greater than the uncoupled wavenumber positions for the two OH···O H-bonds in B15C−H_2O(B) to O(2) and O(4) (3612 cm^{-1}). In keeping with this, the two OH stretch modes of B15C−H_2O(A) are partially localized, with 80% of the displacement of the SS due to motion of the hydrogen in the 2-center hydrogen bond and 80% of the displacement of the AS due to motion of the hydrogen bonded to the aromatic oxygens.

A final remaining question, then, is why the crown−H_2O complexes have splittings between their two water OH stretch fundamentals only one-half to two-thirds of their value in the water monomer? The DFT B3LYP frequency calculations indicate that the OH stretch normal modes are localized on the OH bonds of water, suggesting that motions of the ether oxygens do not contribute to reducing the OH stretch frequencies. Thus the reduced splittings can have contributions from (i) differences in the diagonal force constants of the two OH groups, (ii) changes in the intrabond potential coupling (f_{OH-OH}), and (iii) changes in the kinetic coupling between the two OH bonds. The formation of a singly H-bonded Y···HOH complex, such as occurs in DMB−H_2O, illustrates the typical effect of changing the diagonal force constant of one OH group relative to the other, producing splittings larger than that in the H_2O monomer. In the same way, the 68 cm^{-1} splitting in B15C−H_2O(A), with its inequivalent acceptor sites, is larger than that in B15C−H_2O(B), which has no difference in diagonal force constants. As expected, the sum of kinetic and off-diagonal potential couplings in B15C−H_2O(B) (56 cm^{-1}) is greater than the remaining splitting due to the same causes (31 cm^{-1}) in the asymmetric case in which the two uncoupled OH groups produce a 37 cm^{-1} difference due to the asymmetry of the two acceptor sites (3622−3585 = 37 cm^{-1}).

The kinetic coupling is determined largely by the HOH bending angle, reducing to zero when the two OH bonds are orthogonal to one another. Thus, one reason for the decreased splitting could be a reduction in kinetic coupling associated with a structural change in the H_2O molecule that reduces its intrabond angle in forming the two H-bonds. A study of the SO_2^-−H_2O complex provides precedent for this explanation as the observed splitting of only 40 cm^{-1} was explained by the accompanying decrease in the HOH bond angle (to 96.7°) associated with forming two OH···O hydrogen bonds to the two oxygen atoms of the SO_2 anion.[45] However, if no change in the off-diagonal potential coupling occurred and assuming force constants for an isolated water molecule,[46] interbond angles of ≈98° and 97° for conformers A and B of B15C−H_2O would be required to reduce the observed splittings to 68 and 56 cm^{-1}, respectively. Angular changes of this size are considerably larger than the 2° decrease calculated at the DFT B3LYP/6-31+G(d) level of theory (Table 2). Alternatively, part of the observed splitting could be caused by the off-diagonal intrabond potential coupling ($f_{OH(1)-OH(2)}$). This term also could depend on both the HOH bond angle and the two OH bond lengths. In light of the small calculated change in interbond angle, a Wilson FG matrix analysis[47,48] (described in greater detail in the Supporting Information) predicts that the primary physical mechanism responsible for the observed reduction in the splittings is the reduction in potential coupling between the two OH oscillators when they both bind to the crown ether.

Finally, water complexation also has a significant effect on the spectroscopic signatures of the crown ether, particularly in the changes induced in the alkyl CH stretch spectra. In this region, the spectra are complicated and congested due to contributions from the eight CH_2 groups in B15C and ABC. The spectral signatures of the monomer conformations (see preceding paper)[18] were substantially different for each conformer and robust to substitution of the amino group onto the aromatic ring so that it was possible to use this region to identify structures that shared the same crown conformation.

The most evident difference in this part of the spectrum was the high-frequency region near 2950 cm^{-1}, where sharp transitions were attributed to blue-shifted C−H stretches involved in CH···O interactions. These CH···O interactions have been shown to play an important role in structural stabilization,[49−52] so it is all the more striking that the binding capacity of a single water molecule can open up the crown structure. This open, symmetric structure itself has characteristic spectral signatures in this region, namely that the range of frequencies over which the transitions occur is compressed below 2930 cm^{-1} and the bands are relatively more intense due to the larger dipole changes that can occur from the delocalization of CH stretch modes over the entire crown cycle. These spectral changes may be evident even in room temperature solution, and could serve as a diagnostic of the degree of buckling of the crown.

V. Conclusions

The present study has focused on the preferred binding sites and spectroscopic consequences associated with binding one and two water molecules to the benzo-15-crown-5 ether macrocycle. Two primary binding sites were found, both of which are exposed in a C_s symmetry structure that is the most open structure available to the crown. Interestingly, this open conformation is not among those represented in the expansion-cooled molecule in the absence of the water molecule(s), indicating that even a single water molecule can shift the conformational population distribution entirely from buckled to open. The water molecule(s) take advantage of the oxygen-rich character of the crown ether, donating both its OH groups to H-bonds to the crown oxygens. The two primary binding sites are complementary to one another; one along the long axis of the crown (employing a three-center H-bond to the pair of benzo oxygens and a two-center H-bond to the far outer ether oxygen), and the other perpendicular to this axis, using the remaining two oxygens. The primary B15C−$(H_2O)_2$ structure employs both these sites independently, while a secondary structure has the second water donate a H-bond to the first water in its preferred long-axis orientation. The body of evidence suggests that the 15-crown-5 cycle is nearly ideal in size for binding single water molecule(s), stretching the crown open to do so optimally.

Acknowledgment. We acknowledge the National Science Foundation (CHE-0551075) for financial support of this research. C.W.M. acknowledges the "Deutsche Akademie der Naturforscher Leopoldina" for a postdoctoral scholarship (grant number BMBF-LPD 9901/8-159 of the "Bundesministerium für Bildung und Forschung"). The Rosen Center for Advanced Computing (RCAC) within Information Technology at Purdue and GridChem (http://www.gridchem.org)[53,54] are acknowledged for the computational resources employed for this research. V.A.S. acknowledges Bryan Putnam at RCAC for invaluable advice that aided the completion of the calculations reported herein.

Supporting Information Available: (1) The UV spectroscopy of B15C−H_2O and its comparison with B18C6−H_2O, (2) RIDIR alkyl CH stretch spectra for a larger number of B15C−H_2O conformations, compared with scaled stick spectra from B3LYP/6-31+G(d) harmonic frequency calculations, (3) summary of NH stretch frequency data from experiment and calculation, (4) IR−IR−UV studies of B15C−H_2O and ABC−H_2O, (5) normal modes of CO stretch assigned to be in Fermi resonance with the AS OH stretch transitions, and (6) a Wilson FG matrix analysis of the SS/AS splitting in B15C−H_2O. This material is available free or charge via the Internet at http://pubs.acs.org/JPCA.

References and Notes

(1) Pedersen, C. J. *J. Am. Chem. Soc.* **1967**, *89*, 7017.
(2) Pedersen, C. J. *Science* **1988**, *241*, 536.
(3) Al-Rusaese, S.; Al-Kahtani, A. A.; El-Azhary, A. A. *J. Phys. Chem. A* **2006**, *110*, 8676.
(4) Endicott, C.; Strauss, H. L. *J. Phys. Chem. A* **2007**, *111*, 1236.
(5) Kolthoff, I. M.; Chantooni, M. K. *Can. J. Chem.-Rev. Can. Chim.* **1992**, *70*, 177.
(6) Kumondai, K.; Toyoda, M.; Ishihara, M.; Katakuse, I.; Takeuchi, T.; Ikeda, M.; Iwamoto, K. *J. Chem. Phys.* **2005**, *123*, 024314.
(7) Paulsen, M. D.; Hay, B. P. *J. Mol. Struct.-THEOCHEM* **1998**, *429*, 49.
(8) Wu, Y. J.; An, H. Y.; Tao, J. C.; Bradshaw, J. S.; Izatt, R. M. *J. Inclusion Phenom. Mol. Recognit. Chem.* **1990**, *9*, 267.
(9) Zhelyaskov, V.; Georgiev, G.; Nickolov, Z.; Miteva, M. *Spectrochim. Acta Part a-Mol. Biomol. Spectrosc.* **1989**, *45*, 625.
(10) Kusaka, R.; Inokuchi, Y.; Ebata, T. *Phys. Chem. Chem. Phys.* **2007**, *9*, 4452.
(11) Kusaka, R.; Inokuchi, Y.; Ebata, T. *Phys. Chem. Chem. Phys.* **2008**, *10*, 6238.
(12) Belkin, M. A.; Yarkov, A. V. *Spectrochim. Acta Part a-Mol. Biomol. Spectrosc.* **1996**, *52*, 1475.
(13) ElEswed, B. I.; Zughul, M. B.; Derwish, G. A. W. *J. Inclusion Phenom. Mol. Recognit. Chem.* **1997**, *28*, 245.
(14) ElEswed, B. I.; Zughul, M. B.; Derwish, G. A. W. *Spectrosc. Lett.* **1997**, *30*, 527.
(15) Fukushima, K. *Bull. Chem. Soc. Jpn.* **1990**, *63*, 2104.
(16) Rogers, R. D.; Kurihara, L. K.; Richards, P. D. *J. Chem. Soc., Chem. Commun.* **1987**, 604.
(17) Rogers, R. D.; Richards, P. D. *J. Inclusion Phenom.* **1987**, *5*, 631.
(18) Shubert, V. A.; James, W. H., III; Zwier, T. S. *J. Phys. Chem. A*, preceding article in this issue, DOI: 10.1021/jp904231d.
(19) Shubert, V. A.; Zwier, T. S. *J. Phys. Chem. A* **2007**, *111*, 13283.
(20) Lipert, R. J.; Colson, S. D. *J. Phys. Chem.* **1989**, *93*, 3894.
(21) Page, R. H.; Shen, Y. R.; Lee, Y. T. *J. Chem. Phys.* **1988**, *88*, 4621.
(22) Pribble, R. N.; Zwier, T. S. *Science* **1994**, *265*, 75.
(23) Zwier, T. S. *Annu. Rev. Phys. Chem.* **1996**, *47*, 205.
(24) Halgren, T. A. *J. Comput. Chem.* **1996**, *17*, 616.
(25) Halgren, T. A. *J. Comput. Chem.* **1996**, *17*, 553.
(26) Halgren, T. A. *J. Comput. Chem.* **1996**, *17*, 520.
(27) Halgren, T. A. *J. Comput. Chem.* **1996**, *17*, 490.
(28) Halgren, T. A.; Nachbar, R. B. *J. Comput. Chem.* **1996**, *17*, 587.
(29) Mohamadi, F.; Richards, N. G. J.; Guida, W. C.; Liskamp, R.; Lipton, M.; Caufield, C.; Chang, G.; Hendrickson, T.; Still, W. C. *J. Comput. Chem.* **1990**, *11*, 440.
(30) Becke, A. D. *J. Chem. Phys.* **1993**, *98*, 5648.
(31) Lee, C. T.; Yang, W. T.; Parr, R. G. *Phys. Rev. B* **1988**, *37*, 785.
(32) Moller, C.; Plesset, M. S. *Phys. Rev.* **1934**, *46*, 618.
(33) Frisch, M. J.; Trucks, G. W.; Schlegel, H. B.; Scuseria, G. E.; Robb, M. A.; Cheeseman, J. R.; Montgomery, J. A., Jr.; Vreven, T.; Kudin, K. N.; Burant, J. C.; Millam, J. M.; Iyengar, S. S.; Tomasi, J.; Barone, V.; Mennucci, B.; Cossi, M.; Scalmani, G.; Rega, N.; Petersson, G. A.; Nakatsuji, H.; Hada, M.; Ehara, M.; Toyota, K.; Fukuda, R.; Hasegawa, J.; Ishida, M.; Nakajima, T.; Honda, Y.; Kitao, O.; Nakai, H.; Klene, M.; Li, X.; Knox, J. E.; Hratchian, H. P.; Cross, J. B.; Bakken, V.; Adamo, C.; Jaramillo, J.; Gomperts, R.; Stratmann, R. E.; Yazyev, O.; Austin, A. J.; Cammi, R.; Pomelli, C.; Ochterski, J. W.; Ayala, P. Y.; Morokuma, K.; Voth, G. A.; Salvador, P.; Dannenberg, J. J.; Zakrzewski, V. G.; Dapprich, S.; Daniels, A. D.; Strain, M. C.; Farkas, O.; Malick, D. K.; Rabuck, A. D.; Raghavachari, K.; Foresman, J. B.; Ortiz, J. V.; Cui, Q.; Baboul, A. G.; Clifford, S.; Cioslowski, J.; Stefanov, B. B.; Liu, G.; Liashenko, A.; Piskorz, P.; Komaromi, I.; Martin, R. L.; Fox, D. J.; Keith, T.; Al-Laham, M. A.; Peng, C. Y.; Nanayakkara, A.; Challacombe, M.; Gill, P. M. W.; Johnson, B.; Chen, W.; Wong, M. W.; Gonzalez, C.; Pople, J. A. *Gaussian 03*, revision C.02, revision C.02; Gaussian, Inc.: Wallingford, CT, 2004.
(34) Yi, J. T.; Ribblett, J. W.; Pratt, D. W. *J. Phys. Chem. A* **2005**, *109*, 9456.
(35) Drougas, E.; Philis, J. G.; Kosmas, A. M. *J. Mol. Struct.: THEOCHEM* **2006**, *758*, 17.
(36) Shimanouchi, T. *Tables of Molecular Vibrational Frequencies Consolidated Volume I*; National Bureau of Standards: Gaithersburg, MD, 1972.
(37) Shields, A. E.; Mourik, T. v. *J. Phys. Chem. A* **2007**, *111*, 13272.
(38) Zhao, Y.; Schultz, N. E.; Truhlar, D. G. *J. Chem. Theory. Comput.* **2006**, *2*, 364.

(39) Huang, Z. S.; Miller, R. E. *J. Chem. Phys.* **1989**, *91*, 6613.
(40) Buchanan, E. G.; James, W. H.; Zwier, T. S. Manuscript in preparation.
(41) Al-Jallal, N. A.; Al-Kahtani, A. A.; El-Azhary, A. A. *J. Phys. Chem. A* **2005**, *109*, 3694.
(42) Jagannadh, B.; Kunwar, A. C.; Thangavelu, R. P.; Osawa, E. *J. Phys. Chem.* **1996**, *100*, 14339.
(43) Jagannadh, B.; Sarma, J. A. R. P. *J. Phys. Chem.* **1999**, *103*, 10993.
(44) Paulsen, M. D.; Rustad, J. R.; Hay, B. P. *J. Mol. Struct.: THEOCHEM* **1997**, *397*, 1.
(45) Woronowicz, E. A.; Robertson, W. H.; Weddle, G. H.; Johnson, M. A.; Myshakin, E. M.; Jordan, K. D. *J. Phys. Chem. A* **2002**, *106*, 7086.
(46) Bernath, P. F. *Spectra of Atoms and Molecules*; Oxford University Press: New York, 1995.
(47) Wilson, E. B.; Decius, J. C.; Cross, P. C. *Molecular Vibrations: The Theory of Infrared and Raman Vibrational Spectra*; Dover Publications, Inc: New York, 1955.
(48) Please see Supporting Information.
(49) Hermansson, K. *J. Phys. Chem. A* **2002**, *106*, 4695.
(50) Kar, T.; Scheiner, S. *J. Phys. Chem. A* **2004**, *108*, 9161.
(51) Scheiner, S. *J. Phys. Chem. B* **2006**, *110*, 18670.
(52) Yoshida, H.; Tanaka, T.; Matsuura, H. *Chem. Lett.* **1996**, 637.
(53) Milfeld, K.; Guiang, C.; Pamidighantam, S.; Giuliani, J. *Cluster Computing through an Application-oriented Computational Chemistry Grid;* Proceedings of the 2005 Linux Clusters: The HPC Revolution Linux Clusters Institute, 2005.
(54) Dooley, R.; Allen, G.; Pamidighantam., S. *Computational Chemistry Grid: Production Cyberinfrastructure for Computational Chemistry;* Proceedings of the 13th Annual Mardi Gras Conference Louisana State University, Baton Rouge, LA, 2005.

JP904233Y